THE JOURNAL OF BIOLOGICAL CHEMISTRY VOL. 281, NO. 49, pp. 37720–37727, December 8, 2006

Pre-steady State Electrogenic Events of Ca^{2+}/H^+ Exchange and Transport by the Ca^{2+}-ATPase*

Received for publication, June 23, 2006, and in revised form, October 6, 2006 Published, JBC Papers in Press, October 10, 2006, DOI 10.1074/jbc.M606040200

Francesco Tadini-Buoninsegni[‡], Gianluca Bartolommei[‡], Maria Rosa Moncelli[‡], Rolando Guidelli[‡], and Giuseppe Inesi[§1]

From the [‡]Department of Chemistry, University of Florence, Sesto Fiorentino 50019, Italy and the [§]California Pacific Medical Center Research Institute, San Francisco, California 94107

Native or recombinant SERCA (sarco(endo)plasmic reticulum Ca^{2+} ATPase) was adsorbed on a solid supported membrane and then activated with Ca^{2+} and ATP concentration jumps through rapid solution exchange. The resulting electrogenic events were recorded as electrical currents flowing along the external circuit. Current transients were observed following Ca^{2+} jumps in the absence of ATP and following ATP jumps in the presence of Ca^{2+}. The related charge movements are attributed to Ca^{2+} reaching its binding sites in the ground state of the enzyme (E_1) and to its vectorial release from the enzyme phosphorylated by ATP (E_2P). The Ca^{2+} concentration and pH dependence as well as the time frames of the observed current transients are consistent with equilibrium and pre-steady state biochemical measurements of sequential steps within a single enzymatic cycle. Numerical integration of the current transients recorded at various pH values reveal partial charge compensation by H^+ in exchange for Ca^{2+} at acidic (but not at alkaline) pH. Most interestingly, charge movements induced by Ca^{2+} and ATP vary over different pH ranges, as the protonation probability of residues involved in Ca^{2+}/H^+ exchange is lower in the E_1 than in the E_2P state. Our single cycle measurements demonstrate that this difference contributes directly to the reduction of Ca^{2+} affinity produced by ATP utilization and results in the countertransport of two Ca^{2+} and two H^+ within each ATPase cycle at pH 7.0. The effects of site-directed mutations indicate that Glu-771 and Asp-800, within the Ca^{2+} binding domain, are involved in the observed Ca^{2+}/H^+ exchange.

SERCA (sarco(endo)plasmic reticulum Ca^{2+}-ATPase) is a well characterized cation transport ATPase (1–6) that is obtained with vesicular fragments of sarcoplasmic reticulum (SR).[2] Two Ca^{2+} are transported from the medium into the vesicles, whereas one ATP is utilized. ATPase activation requires binding of two Ca^{2+} per enzyme molecule ($E_1 \cdot 2Ca^{2+}$) followed by ATP utilization and formation of a phosphoenzyme intermediate (E_1-P). The free energy derived from ATP is utilized by the phosphoenzyme for a conformational transition (E_1-P to E_2-P) that favors translocation and release of the bound Ca^{2+} against its concentration gradient. The cycle is completed by hydrolytic cleavage of E_2-P.

Ca^{2+}/H^+ countertransport and electrogenicity were noted (7–9) with native SR vesicles, but most useful information was obtained with reconstituted proteoliposomes (10, 11) that are not leaky to H^+ or other electrolytes. It was then possible to demonstrate that, at neutral pH, the stoichiometry of Ca^{2+}/H^+ countertransport is ~1/1, and because of uneven charge distribution, Ca^{2+} transport is electrogenic (12). The stoichiometric ratio of Ca^{2+}/H^+ exchange varies as the pH outside and inside the vesicles is changed (13), suggesting that the protonation probability of acidic protein residues involved in Ca^{2+}/H^+ exchange varies as E_2-P is formed, whereby H^+ acquisition favors Ca^{2+} dissociation.

A recent contribution (14, 15) derives from continuum electrostatic calculations based on high resolution crystal structures, where E_2 or E_1 ATPase states were stabilized with the high affinity inhibitors (E_2-thapsigargin) or high concentrations of Ca^{2+} ($E_1 \cdot 2Ca^{2+}$). The electrostatic calculations yielded estimates of H^+ occupancy of specific acidic residues in the E_2 and E_1 states of the enzyme and suggested that a minimum of 1.7 and a maximum of 3.0 H^+ are countertransported in a reaction cycle that transports two Ca^{2+} ions.

We have described here pre-steady state charge movements induced by Ca^{2+} concentration jumps in the absence of ATP or by ATP concentration jumps in the presence of Ca^{2+} delivered to Ca^{2+}-ATPase vesicles adsorbed onto an alkanethiol/phospholipid mixed bilayer anchored to a gold electrode (16). This technique has been used in studies of electrogenic transport by several membrane proteins (17–23). In our experiments, the detected charge movements are attributed to the binding of activating Ca^{2+} to the Ca^{2+}-ATPase in the absence of ATP and to translocation of bound Ca^{2+} following the addition of ATP. We have determined the pH dependence of these charge movements and demonstrated unambiguously that the observed electrogenic events correspond to sequential steps within a single enzymatic cycle. We have also demonstrated a different pH dependence of electrogenic signals originating from Ca^{2+} binding to the enzyme in the absence of ATP, as compared with translocation of bound Ca^{2+} following the addition of ATP. This difference is attributed to the variation in the stoichiomet-

* This work was supported by the Ente Cassa di Risparmio di Firenze (PROMELAB Project), the Ministero dell'Istruzione, dell'Università, e della Ricerca, and National Institutes of Health Grant RO1 HL69830. The costs of publication of this article were defrayed in part by the payment of page charges. This article must therefore be hereby marked "*advertisement*" in accordance with 18 U.S.C. Section 1734 solely to indicate this fact.

[1] Recipient of a visiting professorship from the University of Florence (F.S.2.16.04). To whom correspondence should be addressed: California Pacific Medical Ctr. Research Institute, 475 Brannan St., San Francisco, CA 94107. Tel.: 415-6001745; Fax: 415-6001725; E-mail: ginesi@cpmcri.com.

[2] The abbreviations used are: SR, sarcoplasmic reticulum; SSM, solid supported membrane; MOPS, 3-(*N*-morpholino)propanesulfonic acid; WT, wild type.

ric ratio of Ca^{2+}/H^{+} exchange and in the protonation probability (apparent pK_a) of acidic residues in the ground (E_1) and intermediate states (E_2P) of the enzymatic cycle.

MATERIALS AND METHODS

Chemicals—Calcium and magnesium chlorides and MOPS were obtained from Merck at analytical grade. ATP (~97%) and dithiothreitol (≥99% purity) were purchased from Fluka. Octadecanethiol (98%) from Aldrich was used without further purification. EGTA and calcimycin (calcium ionophore A23187) were obtained from Sigma. The lipid solution contained diphytanoylphosphatidylcholine (Avanti Polar Lipids) and octadecylamine (very pure; Fluka) (60:1) it was prepared at a concentration of 1.5% (w/v) in *n*-decane (Merck) as described by Bamberg *et al.* (24).

ATPase Preparations—SR vesicles were obtained from the hind leg muscles of New Zealand White rabbits as described by Eletr and Inesi (25). Recombinant Ca^{2+}-ATPase was obtained from COS-1 cells infected with adenovirus vectors carrying chicken WT (26) or mutant cDNA under the control of the cytomegalovirus promoter (27).

Measurement of Charge Movements—Charge movements were measured by adsorbing the SR vesicles containing the Ca^{2+}-ATPase onto a mixed bilayer anchored to a gold electrode (the so-called solid supported membrane (SSM)). The SSM consisted of an octadecanethiol monolayer covalently linked to the gold surface via the sulfur atom with a diphytanoylphosphatidylcholine monolayer on top of it (28). The gold electrode preparation, the whole experimental setup, as well as the solution exchange technique are described in detail elsewhere (22).

SR vesicles, following a brief sonication in the absence of detergent, were adsorbed on the SSM (usually at an applied potential of +0.1 V, with respect to a Ag/AgCl reference electrode), and the protein was activated by the rapid injection of a solution containing a suitable substrate, *e.g.* Ca^{2+} or ATP, as follows. In Ca^{2+} concentration jump experiments, the "washing" solution contained 150 mM choline chloride, 25 mM MOPS (pH 7.0), 0.25 mM EGTA, 1 mM $MgCl_2$, and 0.2 mM dithiothreitol; the "activating" solution contained, in addition, the required concentration of $CaCl_2$. In ATP concentration jump experiments, the washing solution contained 150 mM choline chloride, 25 mM MOPS (pH 7.0), 1 mM EGTA, 1 mM $MgCl_2$, 1.1 mM $CaCl_2$ (100 μM free Ca^{2+}), and 0.2 mM dithiothreitol; the activating solution contained, in addition, the required concentration of ATP (100 μM). In the case of recombinant Ca^{2+}-ATPase, the concentration jump experiments were carried out by employing the $SURFE^2R^{One}$ device (IonGate Biosciences GmbH, Frankfurt am Main, Germany).

Free Ca^{2+} concentration was calculated with the computer program WinMAXC (29). Unless otherwise stated, 1 μM calcium ionophore A23187 was used to prevent formation of a Ca^{2+} concentration gradient across the SR vesicles (30).

Ca^{2+} Binding, Enzyme Phosphorylation, and Ca^{2+} Transport—Ca^{2+} binding to the ATPase under equilibrium conditions, in the absence of ATP, was measured using a radioactive calcium tracer and EGTA-Ca^{2+} buffers as previously described (31). Pre-steady state enzyme phosphorylation, occlusion of bound Ca^{2+}, and P_i production were measured by adding ATP to enzyme pre-incubated with Ca^{2+} using rapid quench mixers (32). ATP-dependent Ca^{2+} transport was measured by adding ATP to SR vesicles in a medium containing 20 mM pH buffer, 80 mM KCl, 2 mM $MgCl_2$, and 50 μM $CaCl_2$. The loaded vesicles were then vacuum-filtered (Millipore 0.45 μm) after 10–90 s of incubation, and the filters containing the loaded vesicles were washed with 1 mM $LaCl_3$ and processed for determination of radioactive calcium by scintillation counting. Radioactive (^{45}Ca)Ca and (γ-^{32}P)ATP were alternatively used to provide radioactive tracers. The temperature was maintained at 22–23 °C for all of the experiments.

RESULTS

Pre-steady state electrical measurements on an ion pump may yield direct information on charge movements within the transport cycle (16, 33). In our experiments, we activated the pump by delivering Ca^{2+} and/or ATP by a rapid solution exchange procedure, and we detected electrogenic steps by measuring electrical currents along the external circuit. A diagram of our experimental system, with cartoons representing a minimal number of sequential reactions within an ATPase cycle, is shown in Fig. 1. Useful information is gained from current transients. In fact, numerical integration of each transient is related to a net charge movement, which depends upon the particular electrogenic event (*i.e.* following Ca^{2+} or ATP concentration jumps). In addition, kinetic information may be obtained by fitting the current *versus* time curves to a sum of exponentially decaying terms (33).

A current transient induced by a Ca^{2+} concentration jump in the absence of ATP at pH 7 is shown by curve *a* in Fig. 2. This transient is due to binding of Ca^{2+} to the cytoplasmic side of the pump (the exterior of the vesicles), which creates a difference in potential across the vesicular membrane, positive in the direction of the metal support. To keep the applied voltage constant across the whole system, the experimental variation of potential across the vesicular membrane is compensated for by an equal and opposite potential difference across the octadecanethiol-phosphatidylcholine mixed bilayer. This potential difference is produced by a flow of electrons along the external circuit toward the electrode surface. Curve *b* in Fig. 2 shows a current transient induced by an ATP concentration jump at pH 7 in the presence of Ca^{2+} (*i.e.* on Ca^{2+}-ATPase vesicles pre-equilibrated with Ca^{2+}). Here also, the release of the pre-bound Ca^{2+} ions into the vesicle interior (the luminal side) induced by ATP creates a potential difference, again positive toward the metal, which is compensated for by an electron flow along the external circuit. Following the first cycle, when steady state conditions are attained, the flow of Ca^{2+} ions out of the vesicles (favored by a Ca^{2+} ionophore) becomes equal to their flow into the vesicles because of continuous pumping. Under these conditions, the potential difference across the vesicular membrane becomes constant, and consequently, no further signal is detected. In fact, the current flowing along the external circuit (induced by changes in the transmembrane potential) vanishes, whereas the pump current attains its stationary value. The current recorded with the SSM technique is, therefore, different from that recorded with a bilayer lipid membrane incorporating the pump; the former is a measure of the rate of change of the

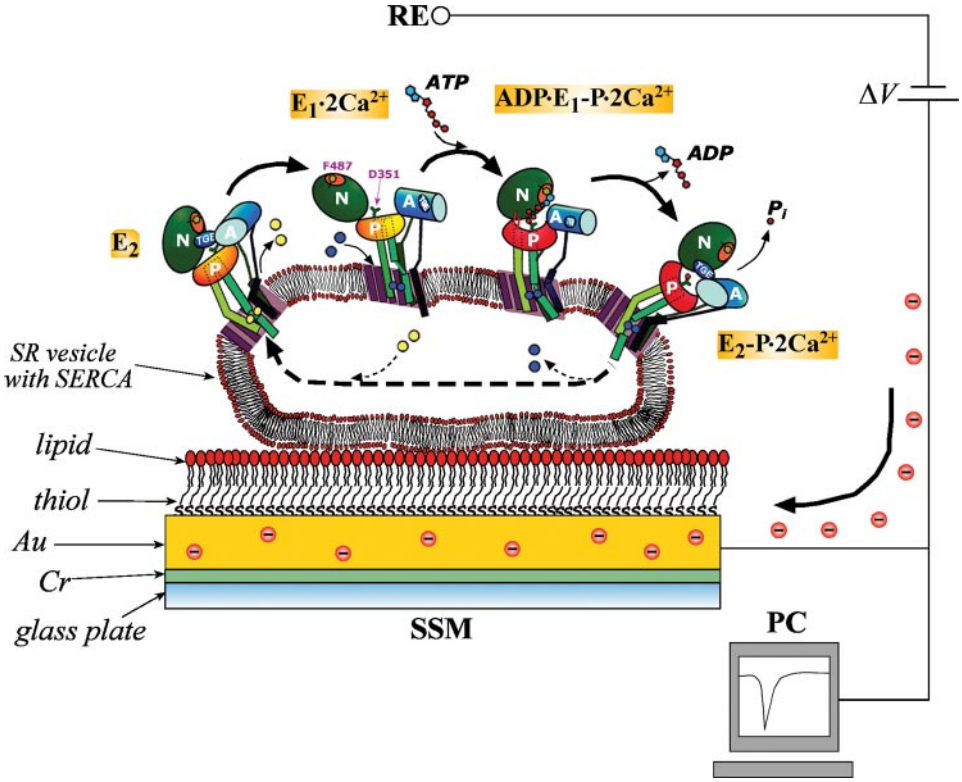

FIGURE 1. **Schematic diagram of a SR vesicle adsorbed on a SSM.** The schematic shows the Ca^{2+}-ATPase undergoing conformational transitions (adapted from Ref. 46) as well as binding and dissociation of Ca^{2+} and H^{+}. In reality, the density of ATPase units within a SR vesicle is much higher than shown in the diagram (36). Nucleotide-binding (*N*), actuator (*A*), and phosphorylation (*P*) domains are indicated together with the TGE region, the adenosine binding (*F487*) and the phosphorylation sites (*D351*). *RE* is the Ag/AgCl reference electrode. When electrogenic transport does occur, a compensating current flows along the external circuit (the *red spheres* are electrons) if the potential difference (Δ*V*) applied across the whole system is kept constant. Consequently, a current transient is recorded through a computer controlled setup (*PC*).

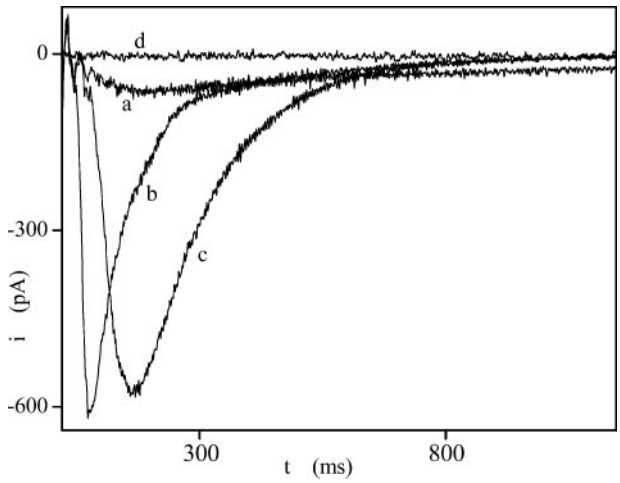

FIGURE 2. **Current transients induced by a 10 μM free Ca^{2+} concentration jump in the absence of ATP (*a*), a 100 μM ATP concentration jump in the presence of 10 μM free Ca^{2+} (*b*), a simultaneous ATP and Ca^{2+} concentration jump (*c*), and a 100 μM ATP concentration jump in the absence of Ca^{2+} (*d*).** *i*, currents; *t*, time.

transmembrane potential, whereas the latter measures the pump current. Voltage-dependent stationary pump currents were recorded by Eisenrauch and Bamberg (34) upon incorporating Ca^{2+}-ATPase directly into a bilayer lipid membrane.

In a previous work (22), we have shown that the SSM current vanishes within a fraction of a second time frame. Thus, jumps of ATP concentrations ranging from 1.5 to 100 μM carried out on Ca-ATPase in the presence of 100 μM free calcium generate current transients whose peak currents increase with ATP concentration following the Michaelis-Menten equation (21, 22). Even though the rate of ATP binding to the pump varies to an appreciable extent, the charge obtained by the integration of these current transients remains constant and may be attributed to the overall amount of Ca^{2+} ions translocated by the pumps in the first cycle.

The current transient induced by a simultaneous concentration jump of ATP and Ca^{2+} is shown by curve *c* in Fig. 2. Integration of transient *a* yields a charge (~50 pCi) that is not particularly accurate, because the current does not vanish completely in 1 s. Integration of the current transients *b* and *c* can be performed more accurately, and yields 93 and 150 pCi, respectively. It is clear that the current transient *c* is practically the sum of the current transient *a* induced by a Ca^{2+} concentration jump on Ca^{2+}-ATPase in the absence of ATP and the current transient *b* induced by an ATP concentration jump on Ca^{2+}-ATPase pre-equilibrated with Ca^{2+}. Subtracting the charge under transient *b* from that under transient *c* yields 57 pCi; this value is more accurate than that (50 pCi) obtained by direct integration of transient *a* and can be regarded as the charge under the current transient generated by binding of Ca^{2+} to the cytoplasmic sites. From a kinetic standpoint, it is also apparent that curve *c* includes the *b* component preceded by the *a* component. It is most important to realize that a 100 μM ATP concentration jump in the absence of Ca^{2+} (Fig. 2, curve *d*) yields no electrogenic signal. We now consider these events in greater detail.

Ca^{2+} Concentration Jumps—A Ca^{2+} concentration jump (in the absence of ATP), performed with the SSM-based technique by rapid injection of Ca^{2+}, yields a current transient (Fig. 3, *Ca^{2+}*) that can be ascribed to Ca^{2+} binding to the ATPase. Identical current transients were obtained in the absence and in the presence of a Ca^{2+} ionophore, indicating that only initial binding to the cytoplasmic side of the protein is involved. Subsequent addition of a Ca^{2+}-chelating solution (containing EGTA) produces dissociation of bound Ca^{2+} revealed by a reverse "off current." The off-current transients (Fig. 3, *EGTA*) are better defined than the on-current transients and allow a more accurate estimate of the corresponding charge by numerical integration over time.

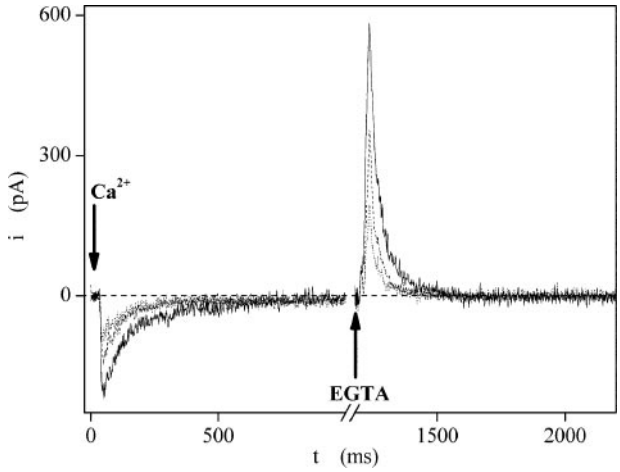

FIGURE 3. **Current transients induced by rapid increase (Ca^{2+} influx) and decrease (EGTA influx) of Ca^{2+} concentration.** Free Ca^{2+} concentrations following the calcium jump are 0.67 μM (*dotted curve*), 2.0 μM (*dashed curve*), and 10.7 μM (*solid curve*). Proceeding toward increasing Ca^{2+} concentrations, the charges obtained by integration of the on currents amount to 9, 16, and 29 pCi, and those obtained by integration of the corresponding off currents amount to 11, 19, and 32 pCi.

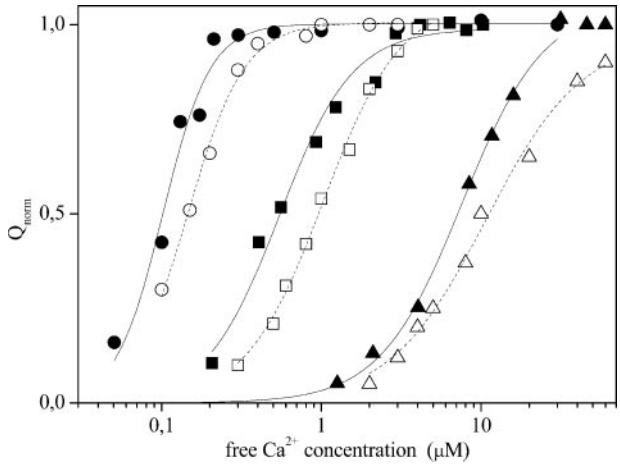

FIGURE 4. **Charges under the current transients following Ca^{2+} concentration jumps at pH 6. 0 (▲, △), 7.0 (■, □), and 8.0 (●, ○) as a function of free Ca^{2+} concentration.** The free Ca^{2+} concentration was obtained with a Ca^{2+}-EGTA buffer. In each curve, these charges (*Q norm*) are normalized with respect to the maximal charge observed at saturating Ca^{2+} at the same pH. The *empty symbols* represent values obtained by direct measurements of Ca^{2+} binding by the use of radioactive tracer under equilibrium conditions (31), whereas the *filled symbols* refer to measurements performed with the SSM-based technique. The *solid* and *dashed curves* are fits of the plots to the Hill equation.

Plots of the charges under the current transients against the concentration of added Ca^{2+} are shown in Fig. 4 at three different pH values, yielding Ca^{2+} binding isotherms quite similar to those obtained by direct measurements of Ca^{2+} binding to SR vesicles in suspension under equilibrium conditions. The binding affinity is higher as the pH is raised from 6.0 to 8.0, as shown by the shift of the curves toward lower Ca^{2+} concentrations, demonstrating the same pattern in both sets of experiments.

Fig. 4 was obtained by plotting the charges under the current transients at various Ca^{2+} concentrations normalized with reference to the maximum charge attained at saturating Ca^{2+} for each pH. The *solid* and *dashed curves* in Fig. 4 are fits of the plots to the Hill equation, and the plots are consistent with the

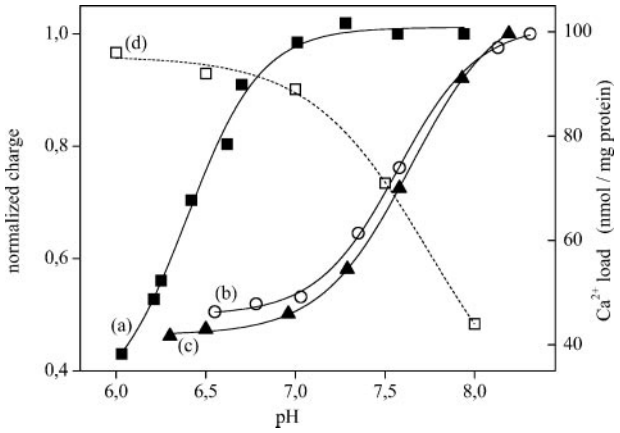

FIGURE 5. **Charges under the current transients following saturating Ca^{2+} concentration jumps (■) and saturating ATP concentration jumps in the presence (○) and in the absence (▲) of Ca^{2+} ionophore as a function of pH.** In each curve, these charges are normalized with respect to the maximal charge attained at alkaline pH. The effect of pH on the maximal levels of Ca^{2+} transported into the SR vesicle upon the addition of ATP (□) is also shown.

known cooperativity of binding. Most importantly, we found that the net moved charge obtained with saturating Ca^{2+} increases from acidic pH values up to pH 7 and then remains constant up to pH 8.0, as shown by plot *a* in Fig. 5. This indicates that charge movement by Ca^{2+} binding is counterbalanced to an appreciable extent by exchange with H^{+} at acidic pH but not at neutral or alkaline pH.

The favorable definition of the off-current transients (Fig. 3, *EGTA*) allows fitting to a multiexponential function, yielding two distinct relaxation rate constants of 33 and 10 s^{-1}, which are probably related to sequential dissociation of the two bound Ca^{2+} ions from the cytoplasmic side of the ATPase. This is in agreement with the stacking modality of the two Ca^{2+} per ATPase molecule (31) and with the two distinct rate constants for Ca^{2+} binding to the ATPase observed with a fluorescent probe (35).

ATP Concentration Jumps—An ATP concentration jump in the presence of saturating Ca^{2+} produces a current transient due to electrogenic Ca^{2+} dissociation from the phosphoenzyme on the luminal side of the SR membrane. Because the K_m value for ATP is 2.9 μM (22), we added 100 μM ATP to ensure a saturating substrate concentration. Fig. 6 shows two current transients induced by ATP jumps in the absence (curve *a*) and in the presence (curve *b*) of a Ca^{2+} ionophore. The current transient in curve *a* decays more rapidly than that in curve *b*, and the underlying charge is smaller. In fact, in the absence of ionophore, the high density of ATPase units in the SR vesicle (36) and the limited luminal volume of the vesicle contribute to a rapid rise of luminal Ca^{2+} with consequent "back inhibition" and blocking of further dissociation of bound Ca^{2+}. Conversely, the presence of ionophore prevents rapid saturation of the vesicle by Ca^{2+}, and the pump is allowed to operate under turnover conditions. In this case, we detect the electrogenic signal generated by the first cycle undergone by the entire population of ATPase molecule. Subsequent stationary currents are not detected by the SSM technique.

The time frame of the current transient produced by the addition of ATP to SR vesicles adsorbed on the SSM (Fig. 6,

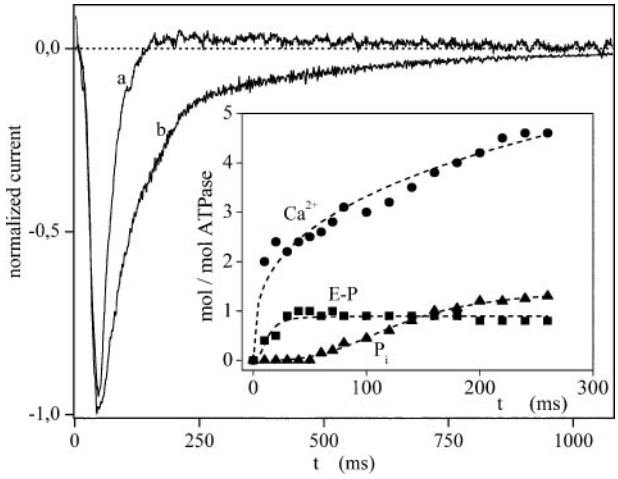

FIGURE 6. **Current transients induced by 100 μM ATP concentration jumps in the absence (*a*) and in the presence (*b*) of a Ca^{2+} ionophore.** The *inset* shows pre-steady state measurements of phosphoenzyme formation (■), Ca^{2+} occlusion and translocation (●), and P_i production by phosphoenzyme cleavage (▲) following the addition of ATP to enzyme pre-equilibrated with Ca^{2+}. The pre-steady state kinetic measurements were obtained with native SR vesicles using radioactive tracers and rapid mixing/quenching instrumentation as previously described (32). *t*, time.

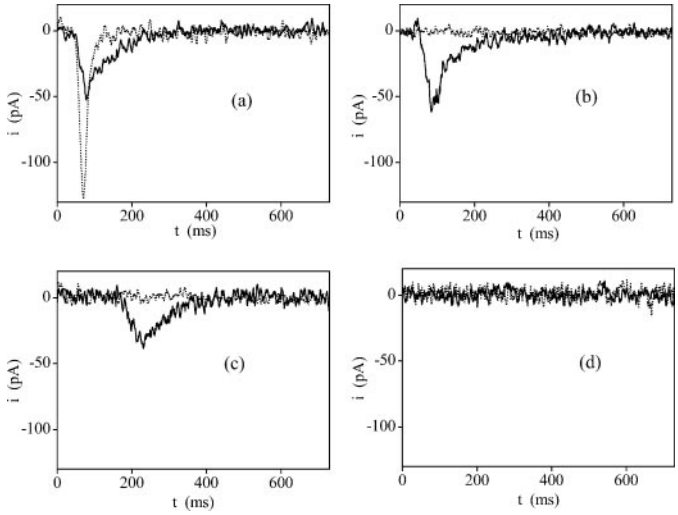

FIGURE 7. **Recombinant WT and mutant ATPase.** Current transients induced by a 10 μM free Ca^{2+} concentration jump in the absence of ATP (*solid curve*), and a 100 μM ATP concentration jump in the presence of 10 μM free Ca^{2+} (*dotted curves*). Shown are WT ATPase (*a*), D351N (*b*), E309A (*c*), and E771Q (*d*) mutants. *i*, currents; *t*, time.

curve *b*) is comparable with that of the first cycle obtained by the addition of ATP to a suspension of SR vesicles in a rapid mixing apparatus. In fact, it is shown in Fig. 6, *inset*, that the first cycle triggered by simultaneous activation of the ATPase molecules upon the addition of ATP is completed in ~150 ms, including enzyme phosphorylation (1 mol/mol), occlusion and translocation of bound Ca^{2+} (2 Ca^{2+}/mole ATPase), and phosphoenzyme cleavage (1 mol P_i/ATPase). The kinetic analogy of the electrogenic and biochemical measurements is related to the use of vesicles and the addition of ATP by rapid mixing in both cases. Steady state turnover of the ATPase in these preparations is 6–8 s^{-1} at 20 °C, which is consistent with the time frame of the first cycle.

If we compare currents obtained in the presence (Fig. 5, curve *b*) or in the absence of ionophore (Fig. 5, curve *c*), we find that the pH dependence of the translocated charge is practically identical under these two conditions but clearly different from the pH dependence of charge movements induced by Ca^{2+} jumps in the absence of ATP (Fig. 5, curve *a*). This indicates that, in both cases, the pH dependence of the current obtained by ATP jumps is related to dissociation of bound Ca^{2+} from the phosphoenzyme.

The pH dependence of the current transients following ATP jumps indicates that charge movements related to Ca^{2+} release from E_2P are counterbalanced by significant H^+ binding at acidic and neutral pH but progressively less at alkaline pH. Comparing the diverse pH dependence of the charges under the current transients after (saturating) Ca^{2+} or ATP jumps (Fig. 5) and considering that the net magnitude of the electrogenic signal is dependent on the ratio of Ca^{2+}/H^+ exchange, it is apparent that, following ATP utilization, the protonation probability of the pertinent acidic residues is increased (*i.e.* their apparent pK_a is shifted to more alkaline pH) as the enzyme undergoes the conformational change from E_1P to E_2P. To evaluate this effect on the ability of the ATPase to unload bound Ca^{2+} from E_2P, we then measured the steady state levels of luminal Ca^{2+} that are reached by active transport at different pH values. These levels are limited by the dissociation constant of the internal phosphoenzyme sites as luminal Ca^{2+} increases because of active transport. It is shown in Fig. 5, curve *d*, that the levels of accumulated Ca^{2+} are significantly reduced as the pH is raised to 8, indicating that, under conditions limiting exchange with H^+ following ATP utilization, Ca^{2+} is less likely to dissociate from E_2P.

Effects of Site-directed Mutations—The relatively high yield of recombinant ATPase from COS-1 cells infected with adenovirus vectors carrying WT or mutant cDNA (27, 37) rendered possible studies on the effects of site-directed mutations on electrogenic signals produced by Ca^{2+} and ATP jumps. It is shown in Fig. 7*a* that the electrogenic signals obtained by concentration jumps of Ca^{2+} and ATP on recombinant WT ATPase display the same pattern as previously observed with native ATPase (Fig. 2). We then tried the effect of Asp-351 mutation. Asp-351 is the residue receiving the γ-phosphate of ATP at the catalytic site to form the phosphorylated intermediate. Its mutation produces catalytic inactivation, even though Ca^{2+} binding is retained. Accordingly, we found that the D351N mutant yields an electrogenic signal upon Ca^{2+} jumps but no signal at all upon ATP jumps in the presence of Ca^{2+} (Fig. 7*b*).

The effects of specific mutations on Ca^{2+} binding were previously studied in detail (38, 39). In our experiment, we first tried the effect of a Glu-309 mutation. Glu-309 resides on Ca^{2+} site II, and its mutation interferes with binding of the second Ca^{2+}, whereas non-cooperative binding of the first Ca^{2+} is retained (37). Because of a strict requirement for occupancy of site II, the enzyme is not able to utilize ATP following Glu-309 mutations. In our experiments, we found that an electrogenic signal was generated by the addition of Ca^{2+}, although within a significantly slower time frame (Fig. 7*c*) as compared with WT or D351N mutant (Fig. 7, *a* and *b*). The evidently slower charge

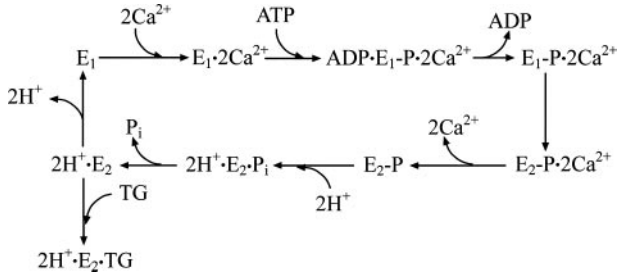

FIGURE 8. **Sequence of partial reactions in the Ca^{2+}-ATPase enzymatic cycle at pH 7. 0.** This is a slight modification of the scheme of de Meis and Vianna (47) and includes H^+ binding as proposed by Butscher *et al.* (48). $2H^+$-E_2-thapsigargin is the dead-end complex produced by thapsigargin (49). Of the states listed in this scheme, high resolution structures for $E_1{\cdot}2Ca^{2+}$, E_2-thapsigargin, and analogs of $ADP{\cdot}E_1{-}P{\cdot}2Ca^{2+}$ and E_2-P were obtained by crystallography (41, 42, 46, 50–52).

movement may be due to interference (by the E309A mutation) with Ca^{2+} entry into the binding cavity (40). No signal was obtained with the E309A mutant following ATP jumps in the presence of Ca^{2+} (Fig. 7*c*).

Finally, we tried the effect of a Glu-771 mutation. Glu-771 is located in Ca^{2+} site I, and because of the tight cooperativity of the Ca^{2+} binding mechanism, its mutation interferes with binding of both Ca^{2+}. In fact, we observed no electrogenic signal upon the addition of Ca^{2+} or ATP to the E771Q mutant (Fig. 7*d*), demonstrating a direct relationship of the electrogenic signals with Ca^{2+} binding.

DISCUSSION

We have reported pre-steady state charge movements within a Ca^{2+}-ATPase cycle obtained with ATPase protein adsorbed on a SSM and subjected to Ca^{2+} jumps in the absence of ATP or to ATP jumps in the presence of Ca^{2+}. In Fig. 5, the charges under the current transients, observed upon Ca^{2+} binding from the cytoplasmatic side in the absence of ATP and upon Ca^{2+} dissociation into the lumen of the vesicles following the addition of ATP, are normalized to their maximum value. This value corresponds to two Ca^{2+} bound and transported per cycle as determined by biochemical measurements (Fig. 6, *inset*). We then estimated the stoichiometry of Ca^{2+}/H^{+} exchange at any given pH by using the values obtained in the same SSM experiments. The pH dependence shown in Fig. 5 indicates that, at pH 7, cooperative binding of two Ca^{2+} ions from the cytoplasmic side takes place without H^+ exchange. This defines the E_1 state, as shown in the diagram of Fig. 8, and implies that the E_1/E_2 equilibrium is pH-dependent. On the other hand, release of the bound Ca^{2+} into the lumenal side following ATP jumps is accompanied by exchange with two H^+ ions. Therefore, the charge of 93 pCi under curve *b* in Fig. 2, generated following the addition of ATP, involves dissociation of two Ca^{2+} ions and exchange of two H^+ ions and, hence, movement of two electronic charges. On the other hand, the charge of 57 pCi (curve *a*) is associated with the movement of two Ca^{2+} ions across a fraction x of the membrane domain of the pump with no H^+ exchange (*i.e.* four charges). Therefore, $4x$ is to 57 pCi as 2 is to 93 pCi; this yields an x value of 0.31. Differently stated, these results indicate that the Ca^{2+} binding sites are located in the membrane domain at ~30% of the membrane thickness from the cytoplasmic side. These conclusions agree with the three-dimensional structure of the Ca-ATPase (41, 42).

Ca^{2+} binding in the absence of ATP occurs with a cooperative mechanism involving sequential occupancy of two neighboring sites (31). The amino acids involved in Ca^{2+} binding within the membrane-bound region of the ATPase were identified by mutational analysis (43). High resolution structures of the Ca^{2+} binding sites were then obtained by crystallography (41, 42). Related atomic models reveal that, in addition to backbone carbonyl oxygens, two water molecules, the Thr-799 side chain, and four acidic residues (Glu-309, Glu-771, Asp-800, and Glu-908) are involved in binding two Ca^{2+} ions. Glu-771 and Asp-800 have very low probability of retaining protons while participating in Ca^{2+} complexation (14, 15). On the other hand, Glu-309 and Glu-908 may retain their protons even in the presence of bound Ca^{2+}, as they are involved in stabilization of local structure by hydrogen bonding.

In the absence of ATP, the electrogenicity of the Ca^{2+} binding step increases as the pH is raised from 6.0 to 7.0 and does not increase any further beyond pH 7.0 (Fig. 5). This variation of net charge movement is related to the H^+ stoichiometry available for exchange upon Ca^{2+} binding with an apparent pK_a value within the 6–7 pH range (Fig. 5). At higher pH values, the carboxyl groups of these residues are completely deprotonated, and no exchange with H^+ occurs to compensate for the charge introduced by Ca^{2+} binding. A pH-dependent equilibrium (Fig. 8) between E_2 (with protonated acidic residues at pH 6.0) and E_1 (with non-protonated acidic residues at pH 7.0) states is consistent with the requirement for enzyme phosphorylation with P_i in the absence of Ca^{2+} (*i.e.* E_2 phosphorylation by P_i in the reverse direction of the pump), which is strongly dependent on acid pH (44).

In the presence of ATP, Ca^{2+} dissociation from the phosphoenzyme is electrogenic at pH 7.0, indicating that compensation by Ca^{2+}/H^{+} exchange is not sufficient to provide complete charge balance at pH 7.0. On the other hand, whereas the signal produced by Ca^{2+} binding in the absence of ATP already reaches its maximal intensity at pH 7.0, the signal produced by Ca^{2+} release following ATP utilization doubles its intensity as the pH is raised from 7.0 to 8.0 (Fig. 5). Therefore, at pH 7.0, the protonation probability of residues involved in Ca^{2+}/H^{+} exchange is increased as a consequence of enzyme phosphorylation. In fact, the moved charge increases 2-fold by raising the pH from 7.0 to 8.0 (Fig. 5) and reaches its maximum at pH 8.0. This indicates that H^+ exchange is totally lacking beyond pH 8, whereby interference with Ca^{2+} transport is observed (Fig. 5). On the other hand, at pH 7.0, H^+ exchange compensates for half the charge moved by two Ca^{2+} ions. Ca^{2+}/H^{+} exchange was previously revealed by steady state rate measurements with proteoliposomes (13). The observed exchange was attributed to countertransport, although H^+ release from nonspecific sites (*i.e.* calsequestrin or others) was not excluded. Presently, our pre-steady state measurements demonstrate directly a 1:1 stoichiometric ratio for Ca^{2+}/H^{+} countertransport (*i.e.* 2.0 H^+/2 Ca^2) within a single cycle at pH 7.0. A 1:2 stoichiometric ratio for Ca^{2+}/H^{+} countertransport is to be excluded, because such a countertransport would be electrosilent and would yield no current transient. In conclusion, our findings indicate that, at

pH 7, two protons are gained from the luminal medium upon release of 2 bound Ca^{2+} ions from the phosphorylated enzyme intermediate. Following P_i release, the two protons are released from the enzyme into the cytoplasmic medium concomitant with the E_2 to E_1 transition, whereupon Ca^{2+} binding from the cytoplasmic side takes place (Fig. 8). We also conclude that, in the physiological transport cycle at pH 7, the protonation probability of the acidic residues participating in Ca^{2+}/H^+ exchange will be very high in E_2-P (apparent pK_a value between pH 7 and 8 (Fig. 5, *b* and *c*), high in E_2 (15), presumably low in E_1, and very low in $E_1{\cdot}2Ca^{2+}$ (Fig. 5*a*) (15).

The results of electrostatic calculations (14, 15) may be helpful in predicting the residues involved in H^+ exchange, as they indicate that protonation of the four relevant transmembrane carboxyl groups is most probable for Glu-771 and then for Asp-800, Glu-309, and Glu-908 in decreasing order of probability. It was also noted (15) that Glu-309 and Glu-908 may retain their protons through the cycle, because of involvement in hydrogen bonding and stabilization of the Ca^{2+}-bound conformation. Our experiments with site-directed mutations (Fig. 7) reveal electrogenic signals following Ca^{2+} jumps on the E309A mutant. Because Ca^{2+} binding on site II does not occur in this mutant, the signal must be attributed to binding on site I. Development of the electrogenic signal then indicates that, at pH 7, the Ca^{2+} charge movement is not neutralized by H^+ release from Glu-771 or Asp-800. Therefore, these residues are dissociated at neutral pH, as the enzyme resides in the E_1 state to favor Ca^{2+} binding (Fig. 8). It is then likely that Glu-771 and Asp-800 are involved in the acquisition of H^+ upon dissociation of Ca^{2+}, as their protonation probability increases as a consequence of conformational changes upon enzyme phosphorylation.

Finally, we consider that replacement of Ca^{2+} with H^+ as well as introduction of water molecules may have an important role in stabilizing the enzyme structure in the E_2 state (14, 15). In addition, our pre-steady state measurements demonstrate that the protonation probability (*i.e.* apparent pK_a) of acidic residues is altered during the ATPase cycle to favor the acquisition of Ca^{2+} in the ground state of the enzyme and exchange of the bound Ca^{2+} with H^+ in E_2-P. These reversible shifts in H^+ acquisition sustain a mechanistic role in promoting dissociation of bound Ca^{2+}. They are produced by changes of H^+ accessibility and/or alterations of the electrostatic environment resulting from long range conformational changes triggered by utilization of ATP. In fact, we show in Fig. 5 that a reduction of H^+ exchange, as the pH is increased to 8, places a limit to Ca^{2+} dissociation from the phosphoenzyme and to the Ca^{2+} concentration that can be reached in the lumen of the vesicles. A sequence of partial reactions within a Ca^{2+}-ATPase cycle, as required to explain our findings, is shown in Fig. 8. Countertransport of H^+ by the Ca^{2+}-ATPase finds an analogy in the mechanism of the Na^+,K^+-ATPase as well as in the structural similarity of the two enzymes (45).

Acknowledgment—We are indebted to Prof. Chikashi Toyoshima for helpful comments and suggestions.

REFERENCES

1. Andersen, J. P., and Vilsen, B. (1995) *FEBS Lett.* **359,** 101–106
2. MacLennan, D. H., Rice, W. J., and Green, N. M. (1997) *J. Biol. Chem.* **272,** 28815–28818
3. MacLennan, D. H., and Green, N. M. (2000) *Nature* **405,** 633–634
4. Inesi, G., and Toyoshima, C. (2004) in *Handbook of ATPases* (Futai, M., Wada, Y., and Kaplan, J. H., eds) pp. 63–87, Wiley-VHC, Weinheim, Germany
5. Toyoshima, C., and Inesi, G. (2004) *Annu. Rev. Biochem.* **73,** 269–292
6. Møller, J. V., Nissen, P., Sørensen, T. L., and Maire, M. (2005) *Curr. Opin. Struct. Biol.* **15,** 387–393
7. Chiesi, M., and Inesi, G. (1980) *Biochemistry* **19,** 2912–2918
8. Meissner, G. (1981) *J. Biol. Chem.* **256,** 636–643
9. Yamagouchi, M., and Kanazawa, T. (1985) *J. Biol. Chem.* **260,** 4896–4900
10. Cornelius, F., and Møller, J. V. (1991) *FEBS Lett.* **284,** 46–50
11. Levy, D., Gulyk, A., Bluzat, A., and Rigaud, J. L. (1992) *Biochim. Biophys. Acta* **1107,** 283–298
12. Yu, X., Carroll, S., Rigaud, J. L., and Inesi, G. (1993) *Biophys. J.* **64,** 1232–1242
13. Yu, X., Hao, L., and Inesi, G. (1994) *J. Biol. Chem.* **269,** 16656–16661
14. Sugita, Y., Miyashita, N., Ikeguchi, M., Kidera, A., and Toyoshima, C. (2005) *J. Am. Chem. Soc.* **127,** 6150–6151
15. Obara, K., Miyashita, N., Xu, C., Toyoshima, I., Sugita, Y., Inesi, G., and Toyoshima, C. (2005) *Proc. Natl. Acad. Sci. U. S. A.* **102,** 14489–14496
16. Pintschovius, J., and Fendler, K. (1999) *Biophys. J.* **76,** 814–826
17. Pintschovius, J., Bamberg, E., and Fendler, K. (1999) *Biophys. J.* **76,** 827–836
18. Tadini-Buoninsegni, F., Nassi, P., Nediani, C., Dolfi, A., and Guidelli, R. (2003) *Biochim. Biophys. Acta* **1611,** 70–80
19. Meyer-Lipp, K., Ganea, C., Pourcher, T., Leblanc, G., and Fendler, K. (2004) *Biochemistry* **43,** 12606–12613
20. Zhou, A., Wozniak, A., Meyer-Lipp, K., Nietschke, M., Jung, H., and Fendler, K. (2004) *J. Mol. Biol.* **343,** 931–942
21. Bartolommei, G., Tadini-Buoninsegni, F., and Moncelli, M. R. (2004) *Bioelectrochemistry* **63,** 157–160
22. Tadini-Buoninsegni, F., Bartolommei, G., Moncelli, M. R., Inesi, G., and Guidelli, R. (2004) *Biophys. J.* **86,** 3671–3686
23. Bartolommei, G., Tadini-Buoninsegni, F., Hua, S., Moncelli, M. R., Inesi, G., and Guidelli, R. (2006) *J. Biol. Chem.* **281,** 9547–9551
24. Bamberg, E., Apell, H. J., Dencher, N. A., Sperling, W., Stieve, H., and Läuger, P. (1979) *Biophys. Struct. Mech.* **5,** 277–292
25. Eletr, S., and Inesi, G. (1972) *Biochim. Biophys. Acta* **282,** 174–179
26. Karin, N. J., Kaprielian, Z., Fambrough, D. M. (1989) *Mol. Cell. Biol.* **9,** 1978–1986
27. Strock, C., Cavagna, M., Peiffer, W. E., Sumbilla, C., Lewis, D., and Inesi, G. (1998) *J. Biol. Chem.* **273,** 15104–15109
28. Seifert, K., Fendler, K., and Bamberg, E. (1993) *Biophys. J.* **64,** 384–391
29. Patton, C., Thompson, S., and Epel, D. (2004) *Cell Calcium* **35,** 427–431
30. Hartung, K., Froehlich, J. P., and Fendler, K. (1997) *Biophys. J.* **72,** 2503–2514
31. Inesi, G., Kurzmack, M., Coan, C., and Lewis, D. E. (1980) *J. Biol. Chem.* **255,** 3025–3031
32. Inesi, G., Coan, C., Verjovshi-Almeida, S., and Lewis, D. (1978) *Ann. N. Y. Acad. Sci.* **307,** 224–227
33. Läuger, P. (1991) *Electrogenic Ion Pumps*, Sinauer Associates Inc., Sunderland, MA
34. Eisenrauch, A., and Bamberg, E. (1990) *FEBS Lett.* **268,** 152–156
35. Peinelt, C., and Apell, H. J. (2005) *Biophys. J.* **89,** 2427–2433
36. Franzini-Armstrong, C., and Ferguson, D. G. (1985) *Biophys. J.* **48,** 607–615
37. Zhang, Z., Lewis, D., Strock, C., Inesi, G., Nakasako, M., Nomura, H., and Toyoshima, C. (2000) *Biochemistry* **39,** 8758–8767
38. Andersen, J. P., and Vilsen, B. (1992) *J. Biol. Chem.* **267,** 19383–19387
39. Andersen, J. P., and Vilsen, B. (1998) *Acta Physiol. Scand. Suppl.* **643,** 45–54
40. Inesi, G., Ma, H., Lewis, D., and Xu, C. (2004) *J. Biol. Chem.* **279,** 31629–31637

41. Toyoshima, C., Nakasako, M., Nomura, H., and Ogawa, H. (2000) *Nature* **405,** 647–655
42. Toyoshima, C., and Nomura, H. (2002) *Nature* **418,** 605–611
43. Clarke, D. M., Loo, T. W., Inesi, G., and MacLennan, D. H. (1989) *Nature* **339,** 476–478
44. Masuda, H., and de Meis, L. (1973) *Biochemistry* **12,** 4581–4585
45. Sweadner, K. J., and Donnet, C. (2001) *Biochem. J.* **356,** 685–704
46. Toyoshima, C., Nomura, H., and Tsuda, T. (2004) *Nature* **432,** 361–368
47. de Meis, L., and Vianna, A. (1979) *Annu. Rev. Biochem.* **48,** 275–292
48. Butscher, C., Roudna, M., and Apell, H. J. (1999) *J. Membr. Biol.* **168,** 169–181
49. Sagara, Y., and Inesi, G. (1991) *J. Biol. Chem.* **266,** 13503–13506
50. Sørensen, T. L., Møller, J. V., and Nissen, P. (2004) *Science* **304,** 1672–1675
51. Toyoshima, C., and Mitsutani, T. (2004) *Nature* **430,** 529–535
52. Olesen, C., Sørensen, T. L., Nielsen, R. C., Møller, J. V., and Nissen, P. (2005) *Science* **306,** 2251–2255

Pre-steady State Electrogenic Events of Ca^{2+}/H^{+} Exchange and Transport by the Ca^{2+}-ATPase

Francesco Tadini-Buoninsegni, Gianluca Bartolommei, Maria Rosa Moncelli, Rolando Guidelli and Giuseppe Inesi

J. Biol. Chem. 2006, 281:37720-37727.
doi: 10.1074/jbc.M606040200 originally published online October 10, 2006
